Hydrol. Earth Syst. Sci. Discuss., 8, 365–390, 2011
www.hydrol-earth-syst-sci-discuss.net/8/365/2011/
doi:10.5194/hessd-8-365-2011

Hydrology and Earth System Sciences Discussions

Impact of climate change on the stream flow of lower Brahmaputra: trends in high and low flows based on discharge-weighted ensemble modelling

A. K. Gain[1,2], W. W. Immerzeel[2,3], F. C. Sperna-Weiland[2], and M. F. P. Bierkens[2,4]

[1]Università Ca' Foscari Venezia, Cannaregio 873, 30121 Venice, Italy
[2]Department of Physical Geography, Utrecht University, P.O. Box 80115, Utrecht, The Netherlands
[3]FutureWater, Costerweg 1G, 6702 AA Wageningen, The Netherlands
[4]Deltares, P.O. Box 80015, 3508 TA, Utrecht, The Netherlands

Received: 22 December 2010 – Accepted: 2 January 2011 – Published: 18 January 2011

Correspondence to: W. W. Immerzeel (w.immerzeel@futurewater.nl)

Published by Copernicus Publications on behalf of the European Geosciences Union.

Abstract

Climate change is likely to have significant effects on the hydrology. The Ganges-Brahmaputra river basin is one of the most vulnerable areas in the world as it is subject to the combined effects of glacier melt, extreme monsoon rainfall and sea level rise. To what extent climate change will impact river flow in the Brahmaputra basin is yet unclear, as climate model studies show ambiguous results. In this study we investigate the effect of climate change on both low and high flows of the lower Brahmaputra. We apply a novel method of discharge-weighted ensemble modeling using model outputs from a global hydrological models forced with 12 different global climate models (GCMs). Based on the GCM outputs and long-term records of observed flow at Bahadurabad station, our method results in a multi-model weighted ensemble of transient stream flow for the period 1961–2100. Using the constructed transients, we subsequently project future trends in low and high river flow. The analysis shows that extreme low flow conditions are likely to occur less frequent in the future. However a very strong increase in peak flows is projected, which may, in combination with projected sea level change, have devastating effects for Bangladesh. The methods presented in this study are more widely applicable, in that existing multi-model streamflow simulations from global hydrological models can be weighted against observed streamflow data to assess at first order the effects of climate change for specific river basins.

1 Introduction

Climate change is likely to lead to an intensification of the global hydrological cycle and to have a major impact on regional water resources (Arnell, 1999). The IPCC Fourth Assessment Report mentions with high likelihood that observed and projected increases in temperature, sea level rise and precipitation variability are the main causes for reported and projected impacts of climate change on water resources, resulting in an overall net negative impact on water availability and the health of freshwater ecosystems (Kundzewicz et al., 2007).

Among the river systems, the hydrological impact of climate change on Ganges-Brahmaputra Basin is expected to be particularly strong. There are three major reasons for this. First, stream flow is strongly influenced by the melt of snow and ice in the upstream part of the catchment. As 60% of the basin area has an elevation of over 2000 m cryospheric processes are deemed important when considering basin hydrology. Projected rise in temperature will lead to increased glacial and snow melt, which could lead to increased summer flows in some river systems for a few decades, followed by a reduction in flow as the glaciers disappear and snowfall diminishes (Immerzeel, 2008). This is particularly true for the dry season when water availability is crucial for the irrigation systems. Immerzeel et al. (2010) stated that the Brahmaputra is most susceptible to reductions of flow, threatening the food security of an estimated 26 million people. Second, the Ganges-Brahmaputra basin is highly influenced by extreme monsoon rainfall and flooding (Mirza, 2002; Warrick et al., 1996). If climate change results in changes of both the intensity and reliability of the monsoon, it will affect both high and low flows leading to increased flooding but possibly also to increased variability of available water, both in space and time (Postel et al., 1996). The latter refers to the fact that discharging water during floods and wet seasons cannot be used during the low flow seasons unless large storage systems are in place (Oki and Kanae, 2006). Third, climate change induced sea level rise results coastal flooding and riverine flooding by causing back-water effect of the Ganges-Brahmaputra basin along the delta (Agrawala et al., 2005).

The objective of this study is to investigate trends in both high and low flow for the lower Brahmaputra river that may arise as a result of climate change. Compared to previous assessments (Warrick et al., 1996; Mirza, 2002; Immerzeel, 2008; Immerzeel et al., 2010) we do not build a basin-specific hydrological model for this purpose. Instead, we use existing results of a global hydrological model that was forced by data from 12 global climate models (GCMs) (Sperna-Weiland et al., 2010) in a weighted ensemble analysis. The novely in this approach lies in that GCM-weights are determined based on the proximity of the associated streamflow simulations to observed streamflow (see

Sperna Weiland et al. (2011) for a first application of this method). Also, the method by which we construct transient stream flow time-series can be considered as novel. Based on the constructed time series of constructed transient stream flow (fore the years 1961–2100) we then project trends in low and high flow statistics for the A1B and A2 emission scenarios.

In remaining part of the paper we first describe the methodology of constructing the transient future time series of river flow in detail. We then show and discuss the results related to the analysis of both low and high flow analysis and conclude the paper by reporting and discussing the major findings.

2 The lower Brahmaputra river basin

The Brahmaputra is a major transboundary river which originates in the glaciated areas of the Kailash range in Tibet (China) at an elevation of 5300 m a.s.l. The river has a length of 2900 km, drains an area of around 530 000 km^2 and traverses four different countries (% of total catchment area in brackets): China (50.5%), India (33.6%), Bangladesh (8.1%) and Bhutan (7.8%). Average discharge of the Brahmaputra is approximately 20 000 $m^3 s^{-1}$ (Immerzeel, 2008). The climate of the basin is monsoon driven with a distinct wet season from June to September, which accounts for 60–70% of the annual rainfall. Immerzeel (2008) categorized the Brahmaputra basin into three different physiographic zones: Tibetan Plateau (TP), Himalayan belt (HB), and the floodplain (FP). These zones respond differently to the anticipated climate change. TP covers 44.4% of the basin, with elevations of 3500 m and above, whereas, HB covers 28.6% of the basin with elevations ranging from 100 m a.s.l to 3500 m a.s.l. The area with an elevation of less than 100 m a.s.l. is considered as FP and comprises about 27% of the entire basin. This study is focusing on river flow in the lower Brahmaputra river basin which belongs to the FP (Fig. 1). In the lower Brahmaputra, average temperature in winter is about 17 °C and summer temperatures on average as high as 27 °C. Total annual precipitation is about 2354 mm concentrated in the monsoon

months June, July, August and September (JJAS). The major discharge measuring station of the lower Brahmaputra is in Bahadurabad (Bangladesh) and long-term observed records from this station will be used to weigh the global hydrological model outputs resulting from the different GCMs.

3 Methods

3.1 Creating an ensemble of discharge time series for the reference period

To investigate the impact of climate change on hydrology we have to rely on combinations of runs of climate models and hydrological effect models. When it comes to climate projectsions, there is no single best model but rather a pool of models or model components that must be interrogated (Knutti, 2008). Projected values of models are inherently uncertain, because a model can never fully describe the physical system and complete confirmation of model output through verification and validation is impossible (Oreskes et al., 1994; Parker, 2006). Therefore, a collection or ensemble of models is preferably used to characterize the uncertainty in projections, while the credibility of projected trends increases when multiple models point in the same direction. Moreover, the average of a multi-model ensemble often outperforms single models when compared with observations (Gleckler et al., 2008; Reichler and Kim, 2008; Knutti, 2008).

This study considers multiple outputs of 12 Global circulation models (GCMs). The output of these GCMs were used to force the global hydrological model PCRGLOBWB. PCR-GLOBWB (van Beek and Bierkens, 2009; Bierkens and van Beek, 2009) calculates for each grid cell ($0.5^{\circ} \times 0.5^{\circ}$ globally) and for each time step (daily) the water storage in two vertically stacked soil layers and an underlying groundwater layer, as well as the water exchange between the layers and between the top layer and the atmosphere (rainfall, evaporation and snow melt). The model also calculates canopy

interception and snow storage. Sub-grid variability is taken into account by considering separately tall and short vegetation, open water, different soil types and the area fraction of saturated soil and the frequency distribution of groundwater depth based on the surface elevations of the 1×1 km Hydro1k data set. Fluxes between the lower soil reservoir and the ground- water reservoir are mostly downward, except for areas with shallow groundwater tables, where fluxes from the ground- water reservoir to the soil reservoirs are possible (i.e. capillary rise) during periods of low soil moisture content. The total specific runoff of a cell consists of saturation excess surface runoff, melt water that does not infiltrate, runoff from the second soil reservoir (interflow) and groundwater runoff (baseflow) from the lowest reservoir. To calculate river discharge, specific runoff is accumulated along the drainage network by means of kinematic wave routing including storage effects and evaporative losses from lakes, reservoirs and wetlands.

In a previous study (Weiland et al., 2010a, b) the output of 12 GCMs (Fig. 2 for names) was used as input to PCR-GLOBWB. Daily precipitation and data to calculate daily reference potential evaporation were collected from the data portal of the Program for Climate Model Diagnosis and Intercomparison (PCMDI) https://esg.llnl.gov:8443/index.jsp. For each GCM model runs for two scenarios, A2 and A1B, were selected that represent the upper range of possible CO_2 emissions. GCM runs comprised the 20C3M control experiment (1971–1990) and the future scenarios A1B and A2 (2081–2100). When multiple ensemble runs were available for one model, the first run was selected. Although the data portal does not provide all required parameters for the Hadley centre climate models, HADGEM1 has been included for it is frequently used in climate change studies. HADGEM1 data has been retrieved from the CERA-gateway, http://cera-www.dkrz.de.

Discharge data were extracted from the model output at the Bahadurabad station, for which also observed discharge data are available from 1973 to 2004. The observed and modelled monthly mean discharges for the overlapping period 1973–1990 are shown in Fig. 2. The figure shows that especially the output of MICRO, GFDL, GISS is similar to the observed data.

3.2 Ensemble weighting based on observed discharge

Rather than statistically downscaling each of the GCMs based on local meteorological data we attached a weight to each of the GCM – PCRGLOB-WB simulated outputs based on a novel method, following Sperna Weiland et al. (2011). Instead of weighting based on similarity of observed GCM-based input (e.g. rainfall), weighting is based on similarity of observed discharge. Using the mean monthly value of observed and simulated discharge during the overlapping period, a weighting factor for each model is computed according to Eq. (1).

$$w_i = \frac{e^{-\frac{1}{12}\sum_{j=1}^{j=12}\frac{(y_j - z_{ij})^2}{\sigma_i^2}}}{\sum_{i=1}^{i=12} e^{-\frac{1}{12}\sum_{j=1}^{j=12}\frac{(y_j - z_{ij})^2}{\sigma_i^2}}}. \quad (1)$$

Where, w is the weighting factor, j is month number, i is model number, σ_i the standard error of discharge observations ($m^3 s^{-1}$), which was assumed to be 25% of the observed value, y_j is the observed average discharge for each month j, and z_{ij} is the mean monthly discharge for model i and month j. The resulting weighting factors for those models with a significant non-zero value are shown in Table 1. It shows that MICRO received the highest value, followed by GFDL, GISS, CCCMA, CGCM, BCCR, NCAR, ECHAM and ECHO.

Using these weighting factors, the daily weighted ensemble average discharge (μ_z) and variance (σ_z^2) can be calculated for the periods of 1961 to 1990 and 2071 to 2100 according to Eqs. (2) and (3).

$$\mu_z = \sum_{i=1}^{i=12} w_i z_i, \quad (2)$$

$$\sigma_z^2 = \sum_{i=1}^{i=12} w_i (z_i - \mu_z)^2 \quad (3)$$

3.3 Construction of a daily transient time series from 1961 to 2100

The 12 GCMs as obtained from the PCMDI used in Sperna-Weiland et al. (2010) only provide runs for time slices (e.g. 1961–1990 and 2071–2100). There are transient runs for some of the GCMs (e.g. at CERA-gateway), but certainly not for all of them. Therefore, to simulate transient time series of discharge for the period 1961–2100, for each of the GCMs the following steps were taken: For each year between 1991 and 2070 a random year is selected either from the reference period or from the projected period. The probability of selecting a random year from the reference period or from the projected period for year i depends on how many years year i is separated from either the reference period or the projected period. For example the probability (P_r) that for the year 2000 a random year is selected from the reference period is 0.88 according to Eq. (4).

$$P_r(i) = 1 - \frac{(i - 1990)}{(i - 1990) + (2071 - i)} \quad (4)$$

Using this approach a complete time series is constructed from 1991 to 2070, resulting in a full time series from 1961–2100. The full time series from 1961 to 2100 is used in the subsequent analysis of trends in high and low flows. Using this approach both statistical properties (year to year variability) as well are preserved in the constructed time series, while trends between time slices, if present, are approximated as being linear with time. It should be noted however that, as we sample discharges directly, we may encounter welding problems between subsequent sampling years: jumps between 31 December and 1 January. However, because we are dealing with a summer Monsoon dominated runoff regime, where low flows occur during boreal winter, such

welding problems are limited. Obviously, in case peak flows occur around the turning of the year, or for rivers with a very strong multi-year component, e.g. due to large groundwater reservoirs, such a construction would not work. In this case, one is required to construct transient meteorological time series first and use these as input to the hydrological model to simulate transient discharge time series.

$$\mu_z = \sum_{i=1}^{i=12} w_i z_i, \tag{5}$$

$$\sigma_z^2 = \sum_{i=1}^{i=12} w_i (z_i - \mu_z)^2 \tag{6}$$

4 Results

4.1 Trends in discharge

Table 2 presents the annual and monthly trends in discharge. From 1961–2100 Trends are calculated by first calculating a trend parameter per GCM and then calculating the weighted mean trend and its variance. From this it can be using a two-sided t-statistic whether a trend is significant or not. Similarly, the explained fraction of variance R^2 is first calculated for each GCM subsequently the weighted average over all models calculated. This analysis was done on both yearly average discharge as well as on discharge per month. Table shows that on annual basis there is a strong positive trend in stream flow that is mainly caused by a strong increase in monsoon discharge. During the dry seasons a modest increase is observed. The only negative trend is found in May, but the correlation is small and the trend non-significant.

Seasonal average flow for both A1B and A2 scenario of four time slices are compared in the box-whisker plots of Fig. 3. Box plots were obtained by first calculating

cumulative frequency distributions per GCM and then constructing a weighted cumulative frequency distribution by weighting values belonging to the same quantile. The statistics in the box plots are thus based on the weighted cumulative frequency distribution. Figure 3 shows that the strongest increase in both average and extreme discharge is predicted for the summer and autumn periods. It also shows that changes in discharge distributions are quite similar between scenarios, except for summer and autumn (i.e monsoon) maximum flows, where the increase is more pronounced for the more extreme A2 scenario. It should however be noted that future spring and early summer discharge may be underestimated as the model does not take into account the increase of melt from glaciers in the upstream parts of the basin, which does play an important role in the Brahmaputra (Immerzeel et al., 2010).

4.2 Flow duration curves

The LBRB is characterized by water shortages in the dry season and water excess and flooding during the monsoon months. To further understand the projected change in range of river discharge, we constructed flow duration curves (Smakhtin, 2001). First for each GCM a flow duration curve was estimated for four 20-year time slices. Next, for each time slice the weighted flow duration curve was calculated by weighting discharge for a given duration. Figures 4 and 5 provide the results for the A1B and A2 scenarios respectively. As can be seen, the Q90 and Q95 flows, commonly used as low flow indices (Pyrce, 2004), remain relatively constant for both scenarios, while the larger changes occur for the larger discharges, i.e. Q25 and up.

4.3 Extreme value analysis

4.3.1 Low flows

Extreme low flow conditions will generally have a negative impact on aquatic ecosystems, agriculture and domestic and industrial sectors. Low flow may occur due to

reduced rainfall, elevated evapotranspiration, reduced water storage or cold temperatures with freezing soils causing a delayed release of melt water (Mauser et al., 2008). A combination of these causes may results in severe low-flow conditions that can impose limitations on above-mentioned sectors, resulting in substantial financial losses.

The low-flow regime of a river can be analyzed in a variety of ways depending on the type of data availability and the type of output information required (Smakthin, 2001; Pyrce, 2004). Here we use the N-day minima approach. Traditionally, the annual minimum (AM) values have been used for low flow frequency analysis, as droughts particularly become an issue when they persist. We use a 7-day low flow frequency using a moving average for the A1B and A2 scenario from 1961 to 2000. Figure 6 shows for four different time slices and two scenario's the relation between return period and 7-day average low flow. Figure 6 is obtained by calculating the 7-day low flow return period per GCM-PCRGLOB-WB model output and subsequently reporting the weighted average of the 12 model outputs. Figure 6 shows a projected decrease in the likelihood of severe low flow events. This is because due to an increase in precipitation that outbalances the increase in evapotranspiration. The differences between the scenarios and time slices increase over time and the A1B scenario yields a stronger increase in low flows than the A2 scenario, which may be related to a less strong decrease in evapotranspiration due to a smaller projected temperature rise.

To show the difference between the 12 models we provide Fig. 7 which shows for the A1B scenario the weighted distribution as a boxplot of yearly average 7-day low flow. Fig. 7 shows that the there is a large variation in low flows between model runs but that all model runs show an increase in 7-day low flow.

4.3.2 High flows

To estimate trends in high flow frequencies we performed a traditional extreme value analysis based on yearly maxima for different time slices. The results are shown in Fig. 8. The graphs are constructed the same way as Fig. 6, but now based on yearly maxima. Figure 8 shows a very strong increase in annual peak flow, which may have

severe impact for flooding in the LBRB. In this case the A2 scenario is the most extreme in line with the steep increase in monsoon precipitation. The 1:10 year discharge is projected to increase from 82 000 $m^3 s^{-1}$ currently to 140 000 $m^3 s^{-1}$ by 2100 and a peak flow that currently occurs every 10 years will occur at least once every two years during the time slice 2080–2099. It is striking that for peak flows with larger return periods the strongest increase already occurs during the first 20 years. This could most likely be attributed to sampling variability resulting from performing the extreme analysis on relatively short 20 year time slices resulting in more than the expected number of randomly selected years from the 2071–2100 time slice. This could be corrected for by performing the analysis repeatedly for each model on multiple transients constructed by Eq. (4).

5 Conclusions and discussions

In this study we applied a new method to construct a daily discharge time series from using a discharge-weighted ensemble based on inputs from 12 GCMs to a global hydrological model. Weighted discharge time series were subsequently used to analyze future trends in average flow and extreme flow results show that climate change is likely to improve dry season conditions in the LBRB. For both scenarios (A1B and A2), for all models and for all time slices both average flow and extreme low flow is projected to increase in size. Low flow conditions may even be slightly underestimated as the accelerated glacial melt in the upstream parts of the catchment may, albeit temporarily, further enhance low flow. The A1B scenario projects the strongest increase in low flow. On the other hand, our analysis also shows a large increase in peak flow size and frequency. The impact for the already highly flood prone plains of Bangladesh may be devastating, in particular in combination with the projected sea level rise. The A2 scenario projects the strongest increase in high flow.

For the assessment of streamflow of Ganges-Brahmaputra basin, previous studies (Warrick et al., 1996; Mirza, 2002; Immerzeel, 2008; Immerzeel et al., 2010) applied

basin-specific hydrological model. Through statistical downscaling of six GCMs and using multiple regression analysis, Immerzeel (2008) found a sharp increase in the occurrence of average and extreme downstream discharge of Brahmaputra for A2 and B2 storylines. Mirza (2002) used climate change scenarios from four GCMs as input into hydrological models and result of the study demonstrates substantial increases in mean peak discharges in the rivers of Ganges-Brahmaputra basin. But in our study, we use existing results of a global hydrological model that was forced by data from 12 global climate models (GCMs) in a weighted ensemble analysis.

The results in this paper show that all GCMs point toward an increase in discharge of the lower Brahmaputra river. However, it should be noted that there is quite some uncertainty about the change in South-Asian Monsoon strength, and most climate models have difficulty simulating mean monsoon characteristics and associated inter-annual precipitation variation (Annamalai et al., 2007; Yang et al., 2008). Experiments with regional climate models even show contradictory results (e.g. Kumar et al., 2006 vs. Ashfaq et al., 2009). However, given all the evidence, an increase in peak flow and flood frequency is likely and adaptive measures should be seriously considered.

In this paper we performed no model simulations of our own. Instead we made use of a repository of existing runs of a global hydrological model forced by a multi-model ensemble of climate data for both a reference period and 2071–2100 projections. By weighting the simulated discharge with discharge observations a multi-model ensemble analysis of climate change effects could be made for a particular location, in this case the lower Brahmaputra at Bahadurabad station. Through this, a form of implicit downscaling is achieved that also takes account of inter-GCM uncertainty. Moreover, the method, which allows for a very quick and cheap analysis of the effects of climate change plus uncertainty, is quite generic and can be used at other locations in the world with discharge observations, provided that the upstream area is large enough (we are dealing with a global hydrological model). The method can be easily improved to allow for the case that none of the models is doing a good job in reproducing discharge by adding bias-correction methods.

Ideally, the hydrological community could make a repository where the results of combinations of different GCMs and different global hydrological models are stored; both reference runs and projections for future time slices. Analyses by the method presented in this paper could then be done very quickly for any large river in the world, but now also taking the uncertainty about hydrological response into account. To have transient runs would be even better, but given that they only available for few GCMs at this time, transient could be constructed for rivers with a strong seasonal signals as in our case. Alternatively, instead of interpolating discharge itself, one could also construct a transient of statistics by first estimating discharge statistics for each time slice and then interpolating changes of these statistics between time slices.

Acknowledgements. Part of this research was conducted while the first author was a guest at the Department of Physical Geography of University of Utrecht.

References

Agrawala, S., Ota, T., Ahmed, A. U., Smith, J., and van Aalst, M.: Development and climate change in Bangladesh: focus on coastal flooding and the Sundarbans, Organisation for Economic Co-operation and Development (OECD), Paris, 2005.

Annamalai, H., Hamilton, K., and Sperber, K. R.: The South Asian summer monsoon and its relationship with ENSO in the IPCC AR4 simulations, J. Climate, 20, 1071–1092, 2007.

Arnell, N. W.: Climate Change and global water resources, Glob. Env. Change, 9, 31–49, 1999.

Ashfaq, M., Shi, Y., Tung, W., Trapp, R. J., Gao, X., Pal, J. S., and Diffenbaugh, N. S.: Suppression of south Asian summer monsoon precipitation in the 21st century, Geophys. Res. Lett., 36, L01704, doi:10.1029/2008GL036500, 2009.

Bierkens, M. F. P. and van Beek, L. P.: Seasonal Predictability of European Discharge: NAO and hydrological response time, J. Hydrometeorol., 10, 953–968, 2009.

Gleckler, P. J., Taylor, K. E., and Doutriaux, C.: Performance metrics for climate models, J. Geophys. Res.-Atmos., 113, D06104, doi:10.1029/2007JD008972, 2008.

Immerzeel, W.: Historical trends and future predictions of climate variability in the Brahmaputra basin, Int. J. Climatol., 28, 243–254, 2008.

Immerzeel, W. W., van Beek, L. P., and Bierkens, M. F. P.: Climate Change Will Affect the Asian Water Towers, Science, 328, 1382–1385, 2010.
IPCC: Summary for Policymakers in: Climate Change 2007: The Physical Science Basis. Contribution of Working Group I to the Fourth Assessment Report of the Intergovernmental Panel on Climate Change, edited by: Solomon, S., Qin, D., Manning, M., Chen, Z., Marquis, M., Averyt, K. B., Tignor, M., and Miller, H. L., Cambridge University Press, Cambridge, UK and New York, NY, USA, 2007.
Knutti, R.: Should we believe model predictions of future climate change?, Philos. T. R. Soc. A, 366, 4647–4664, 2008.
Kumar, K. R., Sahai, A. K., Kumar, K. K., Patwardhan, S. K., Mishra, P. K., Revadekar, J. V., Kamala, K., and Pant, G. B.: High-resolution climate change scenarios for India for the 21st century, Curr. Sci. India, 90, 334–345, 2006.
Kundzewicz, Z. W., Mata, L. J., Arnell, N. W., Döll, P., Kabat, P., Jiménez, B., Miller, K. A., Oki, T., Sen, Z., and Shiklomanov, I. A.: Freshwater resources and their management.Climate Change 2007: Impacts, Adaptation and Vulnerability. Contribution of Working Group II to the Fourth Assessment Report of the Intergovernmental Panel on Climate Change, edited by: Parry, M. L., Canziani, O. F., Palutikof, J. P., van der Linden, P. J., and Hanson, C. E., Cambridge University Press, Cambridge, UK, 173–210, 2007.
Mauser, W., Marke, T., and Stoeber, S.: Climate change and water resources: scenarios of low-flow conditions in the Upper Danube River Basin, IOP Conference Series: Earth and Environmental Science, 4(012027), 1–11, 2008.
Mirza, M. M. Q.: Global warming and changes in the probability of occurrence of floods in Bangladesh and implications, Glob. Env. Change, 12, 127–138, 2002.
Oki, T. and Kanae, S.: Global Hydrological Cycles and World Water Resources, Science, 313, 1068–1072, 2006.
Oreskes, N., Shrader-Frechette, K., and Belitz, K.: Verification, validation, and confirmation of numerical models in the earth sciences, Science, 263, 641–646, 1994.
Parker, W. S.: Understanding pluralism in climate modeling, Foundation of Science, 11, 349–368, 2006.
Postel, S. L., Daily, G. C., and Ehrlich, P. R.: Human appropriation of renewable fresh water, Science, 271, 785–788, 1996.
Pyrce, R.: Hydrological Low Flow Indices and their Uses, WSC Report No. 04-2004, Watershed Science Centre, Peterborough, Ontario, 2004.

Reichler, T. and Kim, J.: How well do coupled models simulate today's climate?, B. Am. Meteorol. Soc., 89, 303–311, 2008.
Smakhtin, V. Y.: Low flow hydrology: a review, J. Hydrol., 240, 147–186, 2001.
Sperna Weiland, F. C., van Beek, L. P. H., Kwadijk, J. C. J., and Bierkens, M. F. P.: The ability of a GCM-forced hydrological model to reproduce global discharge variability, Hydrol. Earth Syst. Sci., 14, 1595–1621, doi:10.5194/hess-14-1595-2010, 2010.
Sperna Weiland, F. C., Beek van, L. P. H., Weerts, A. H., Bierkens, M.F.P.: A comparison of methods for weighting and combining global runoff projections from an ensemble of GCMs: Extracting information from an ensemble of GCMs to reliably assess global future runoff change, J. Hydrol., (submitted), 2011.
Van Beek, L. P. H. and Bierkens, M. F. P.: The Global Hydrological Model PCR-GLOBWB: Conceptualization, Parameterization and Verification, Report, Department of Physical Geography, Utrecht University, available at: http://vanbeek.geo.uu.nl/suppinfo/vanbeekbierkens2009.pdf, 2009.
Warrick, R. A., Bhuiya, A. H., and Mirza, M. Q.: The greenhouse effect and climate change, in: The Implications of Climate and Sea-Level Change for Bangladesh, edited by: Warrick, R. A. and Ahmad, Q. K., Kluwer Academic Publishers, Dordrecht, Briefing Document 1, 1996.
Yang, S., Zhang, Z., Kousky, V. E., Higgins, R. W., Yoo, S.-H., Liang, J., and Fan, Y.: Simulations and Seasonal Prediction of the Asian Summer Monsoon in the NCEP Climate Forecast System, J. Climate, 21, 3755–3775, 2008.

Table 1. Computed weighing factors for the different model forcings.

	MICRO	GFDL	GISS	CCCMA	CGCM	BCCR	NCAR	ECHAM	ECHO
w_i	0.369	0.299	0.200	0.092	0.034	0.003	0.002	0.001	0.001

Table 2. Trends in monthly annual stream flow from 1961 to 2100. Trends and R^2 are first calculated per GCM and subsequently the weighted average calculated. All trends are significant at the 95% confidence level, except for the trend in May discharge for the A2 scenario.

	Trend ($m^3\,s^{-1}\,yr^{-1}$)		R^2	
	A1B	A2	A1B	A2
Yearly Average	39	49	0.45	0.36
January	4	6	0.12	0.21
February	4	4	0.10	0.11
March	11	11	0.27	0.23
April	15	10	0.23	0.10
May	−13	−6	0.03	0.00
June	47	41	0.05	0.06
July	101	138	0.22	0.22
August	166	207	0.39	0.36
September	82	98	0.30	0.31
October	23	45	0.09	0.18
November	15	25	0.14	0.14
December	9	9	0.21	0.17

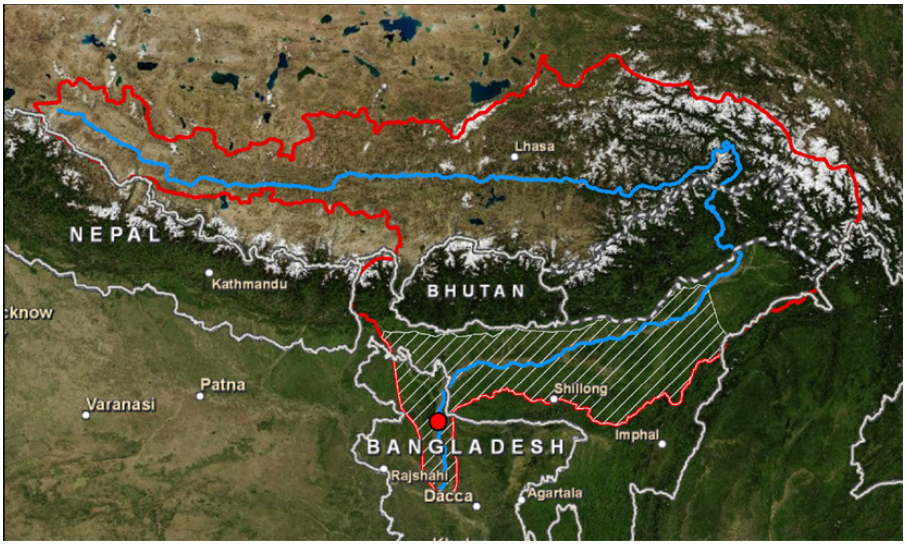

Fig. 1. Overview of the Brahmaputra river basin (red polygon), the Brahmaputra river (blue line), the outlines of the lower Brahmaputra river basin (shaded white) and the Bahadurabad gauging station (red dot).

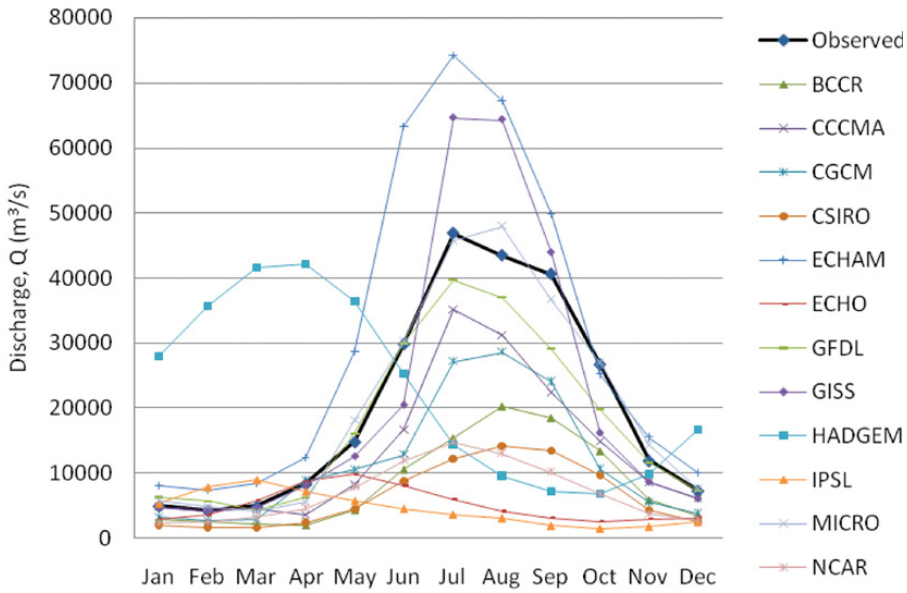

Fig. 2. Comparison of monthly mean discharge as simulated by PCR-GLOBWB with different GCMs as input with that obtained from observed discharge at Bahadurabad station.

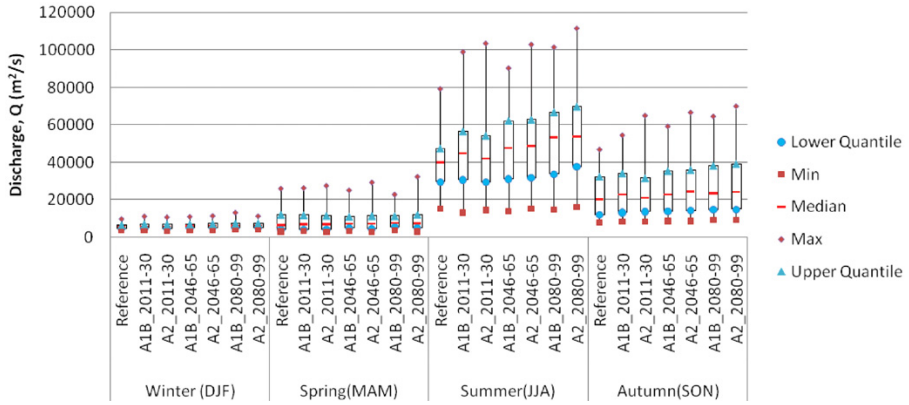

Fig. 3. Box plots of stream flow for different seasons and for different time slices. Box plot represents the multi-model weighted variation over the season.

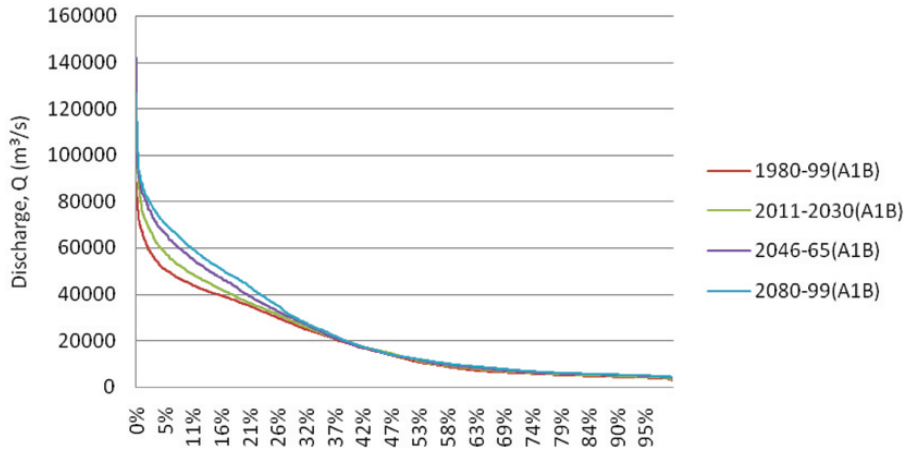

Fig. 4. Multi-model weighted flow duration curve for 4 different time slices for the A1B scenario.

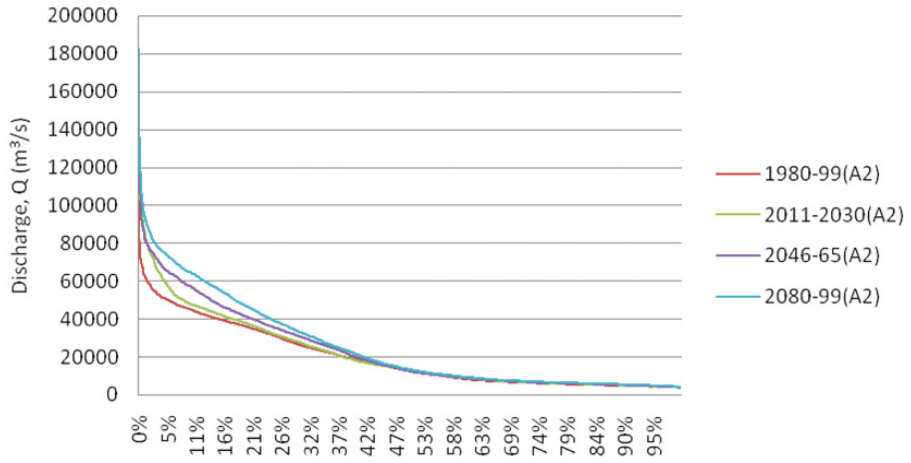

Fig. 5. Multi-model weighthed flow duration curve for 4 different time slices for the A2 scenario.

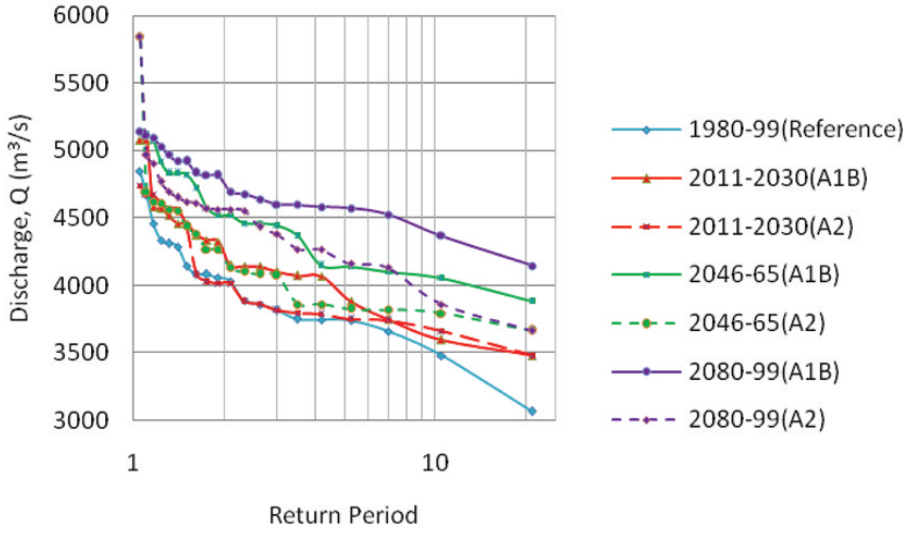

Fig. 6. Seven day low flow for different return periods for different scenario's and time slices as obtained from a weighted average of 12 model outputs.

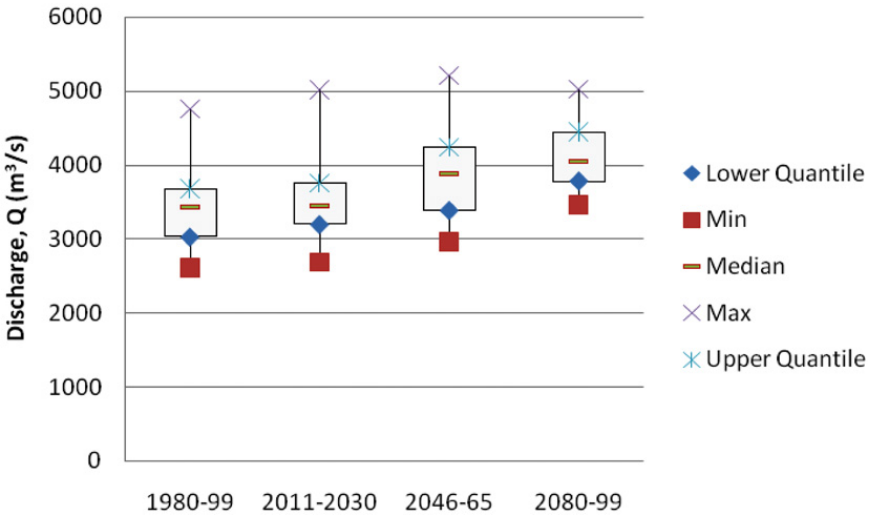

Fig. 7. Box-whisker plot for yearly average 7-day low flow for A1B Scenario of 12 different weighted hydrological model outputs.

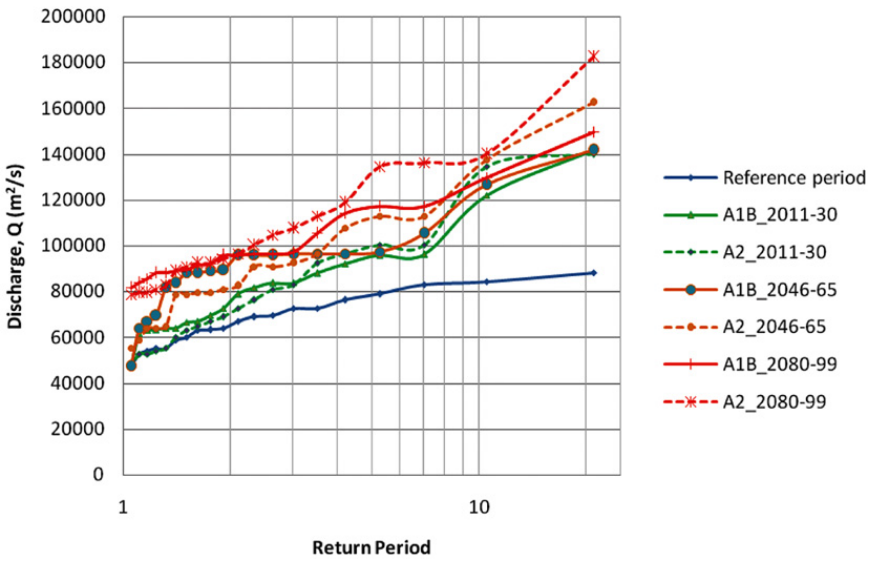

Fig. 8. Annual peak flow for different return periods, time slices and scenario's obtained from a weighted average of extreme value analysis of the 12 model outputs.